PAPER

A sinteractive Ni–BaZr$_{0.8}$Y$_{0.2}$O$_{3-\delta}$ composite membrane for hydrogen separation†

Shumin Fang,[a] Siwei Wang,[ab] Kyle S. Brinkman[b] and Fanglin Chen[*a]

BaZr$_{0.8}$Y$_{0.2}$O$_{3-\delta}$ (BZY) is an excellent candidate material for hydrogen permeation membranes due to its high bulk proton conductivity, mechanical robustness, and chemical stability in H$_2$O- and CO$_2$-containing environments. Unfortunately, the use of BZY as a separation membrane has been greatly restrained by its highly refractory nature, poor grain boundary proton conductivity, high number of grain boundaries resulting from limited grain growth during sintering, as well as low electronic conductivity. These problems can be resolved by the fabrication of a Ni–BZY composite membrane with large BZY grains, which requires the development of a sinteractive Ni–BaZr$_{0.8}$Y$_{0.2}$O$_{3-\delta}$ materials system. In this work, Ni–BZY composite membranes have been fabricated by three methods: (i) a combined EDTA-citric method, (ii) a solid state reactive sintering method, and (iii) a solid state reaction method. The effects of different fabrication methods on the sintering activity, microstructure, and phase composition have been systematically investigated by dilatometry, scanning electron microscopy, and powder X-ray diffraction. After reduction, only Ni–BZY membranes prepared through the solid state reaction method were observed to be dense with large BZY grains ($\sim$1 μm). It has been found that the densification and grain growth of Ni–BZY composite membranes were controlled by the method and sequence of NiO introduction during composite membrane processing. After process optimization, a 0.44 mm-thick Ni–BZY dense composite membrane was fabricated using the solid state reaction method which exhibited a hydrogen flux of 4.3 × 10^{-8} mol cm^{-2} s^{-1} in wet 40% H$_2$ at 900 °C, significantly higher than those of non-BaCeO$_3$-based hydrogen separation membranes.

1 Introduction

Hydrogen is an important raw material for the production of ammonia, methanol, and liquid hydrocarbons. Hydrogen is principally derived from fossil fuels, especially through catalytic steam reforming of methane,[1] which is strongly endothermic and requires high temperature (700–900 °C) to achieve maximum conversion to H$_2$, CO, and CO$_2$ at high pressure (20–40 bar).[2] In this process, high purity hydrogen can then be directly obtained *via* a separation step such as hydrogen permeation through a proton-conducting membrane under a pressure gradient at high temperature. The application of membrane technology is expected to considerably reduce the capital and energy cost in hydrogen production. Conventional Pd-based membranes and amorphous glass materials are not suitable for this process due to the high temperatures (700–

900 °C) required for process efficiency.[3,4] Therefore, alternatives such as composite membranes consisting of a BaCeO$_3$-based proton conductor and an electronic conductor (*e.g.* nickel) have been developed for this application.[5] However, these membranes (*e.g.* Ni–BaZr$_{0.8-x}$Ce$_x$Y$_{0.2}$O$_{3-\delta}$ (Ni–BZCY), 0.4 ≤ x ≤ 0.8) suffered serious performance loss in a wet CO$_2$-containing environment at 900 °C.[6,7] The performance degradation was attributed to the insulating effect of BaCO$_3$ formed by the reaction between BaCeO$_3$ and CO$_2$. In order to avoid the chemical stability issue of BaCeO$_3$, CO$_2$-tolerant hydrogen separation membranes have been developed, *e.g.*, RE$_6$WO$_{12-\delta}$ (RE: rare earth metal), Ca-doped LaNbO$_4$, Ce$_{0.8}$Sm$_{0.2}$O$_{2-\delta}$, and Ni–La$_{0.4875}$Ca$_{0.0125}$Ce$_{0.5}$O$_{2-\delta}$.[8–12] However, the permeation fluxes of those membranes are significantly lower than those of Ni–BZCY membranes due to their low proton conductivity and/or electronic conductivity. Among the proton conductors that are tolerant to CO$_2$, BaZr$_{0.8}$Y$_{0.2}$O$_{3-\delta}$ (BZY) possesses the highest bulk proton conductivity.[13] Unfortunately, a single phase BaZr$_{0.85}$Y$_{0.15}$Mn$_{0.05}$O$_{3-\delta}$ membrane shows very low hydrogen flux (3.0 × 10^{-9} mol cm^{-2} s^{-1} in wet 50% H$_2$ at 900 °C for a 0.9 mm-thick membrane) due to the relatively poor electronic conductivity.[14] The low flux may be resolved in a similar way to composite Ni–BZCY membranes: by combining BZY with highly electronic-conducting Ni to form a Ni–BZY composite membrane.

[a]Department of Mechanical Engineering, University of South Carolina, Columbia, SC 29208, USA. E-mail: chenfa@cec.sc.edu

[b]Department of Materials Science and Engineering, Clemson University, Clemson, SC 29634, USA

This journal is © The Royal Society of Chemistry 2014

J. Mater. Chem. A, 2014, 2, 5825–5833 | 5825

A composite Ni–BZY membrane is expected to possess both high hydrogen permeation flux and chemical stability, which are the key factors for successful adoption of the Ni–BZY hydrogen permeation membrane for practical applications. However, there have been no reports to date on Ni–BZY composite membranes for hydrogen permeation, probably due to the difficulty in obtaining dense membrane with large BZY grains.

Sintering of Ni–BZY membranes needs to be performed below the melting point of Ni (~1453 °C). Unfortunately, due to their highly refractory nature, BZY samples prepared through the traditional solid state reaction method need to be sintered at extremely high temperatures (1700–2100 °C) for a long time (24 h) to reach relatively high density, potentially at the risk of barium evaporation.[15–17] The evaporation of barium will lead to the precipitation of "yttria-like" material and significant degradation of proton conductivity.[18] At a sintering temperature of 1400 °C, the conventional solid state reaction method can only produce BZY with low relative density and small grain size.[19] Moreover, BZY has low grain boundary proton conductivity due to the blocking effect of space charge layers present at the interface.[20–22] The small grain size and large number of grain boundaries will greatly limit the total proton conductivity of BZY. Therefore, significant efforts have been made to achieve dense and large-grained BZY ceramics and minimize interfacial and grain boundary effects.[18,23–27] The proton conductivity of the grain-boundary-free BZY film prepared by pulsed laser deposition is two orders of magnitude higher than that of conventionally sintered BZY samples.[25] However, pulsed laser deposition is not commonly available and may not be suitable for economical fabrication of Ni–BZY membranes for practical applications. Recently, a solid state reactive sintering method has been developed to fabricate dense BZY pellets using 1–2 wt% NiO as the sintering aid.[24,26–28] Highly dense BZY ceramics with a large grain size (up to 5 μm) can be obtained at a relatively low sintering temperature of 1500 °C.[26] This method can be useful in the fabrication of composite Ni–BZY membranes. The sol–gel method has been employed to prepare highly sinteractive BZY powder due to the high sinterability of the nanocrystalline precursor. However, the densification of BZY powders prepared by the sol–gel method still needs a high sintering temperature of 1600 °C using the reactive sintering method.[20] Therefore, it may be difficult to prepare dense Ni–BZY using BZY powders from the sol–gel method. On the other hand, sinteractive NiO–BZY powder can be prepared by the one-pot combustion method.[23,29] The NiO–BZY powder can be reduced to prepare the Ni–BZY powder which is also expected to be sinteractive.

Given the importance of high performance Ni–BZY dense hydrogen permeation membranes and the difficulty in densification of BZY at a low temperature of ~1400 °C, it is of great significance to develop sinteractive Ni–BZY composites by systematically investigating the processing conditions required to achieve dense Ni–BZY membranes with a large grain size. In this work, three different methods including (i) a combined EDTA-citric method, (ii) a solid state reactive sintering method, and (iii) a solid state reaction method were employed aiming at fabricating dense and large-grained Ni–BZY membranes. The sintering behavior, microstructure, and phase composition of

the Ni–BZY from different methods were investigated. Dense Ni–BZY membranes with large BZY grains were successfully achieved through a two-step solid state reaction method. A high hydrogen flux was obtained for the Ni–BZY membrane prepared from this method, suggesting that Ni–BZY composite membranes are a promising material solution for hydrogen permeation.

2 Experimental

Fig. 1 schematically shows the different methods for fabrication of Ni–BZY membranes. Ni–BZY (volume ratio 40 : 60) powders were prepared through a combined EDTA-citric method (CEC), a solid state reactive sintering method (SSRS), and a solid state reaction method (SSR). In the CEC method, Ba(NO$_3$)$_2$ (Alfa Aesar 99%), ZrO(NO$_3$)$_2$·xH$_2$O (Alfa Aesar 99.9%), Y(NO$_3$)$_3$·6H$_2$O (Alfa Aesar 99.9%), and Ni(NO$_3$)$_2$·6H$_2$O (Alfa Aesar 99.9%) were dissolved in deionized water and titrated by ethylenediaminetetraacetic acid (EDTA). Stoichiometric amounts of metal nitrate solutions (weight ratio NiO : BZY = 1 : 1) were mixed in a beaker and heated at 80 °C under stirring. EDTA and citric acid (CA) were added as chelating agents, with the molar ratio of EDTA/citric acid/total metal cations at 1 : 1.5 : 1. The pH value of the solution was adjusted by ammonia additions to a value of approximately 8. An appropriate amount of ammonium nitrate was then added to trigger combustion. The solution was heated until self-ignition to obtain NiO–BZY powder, which was then calcined at 1100 °C for 10 h followed by reduction in 5% H$_2$/N$_2$ at 1000 °C for 5 h to obtain Ni–BZY20-CEC powder. BZY20 powder was also prepared by this method and calcined at 1100 °C for 10 h (denoted as BZY20-CEC). In the SSRS method, stoichiometric amounts of BaCO$_3$ (Alfa Aesar 99.8%), ZrO$_2$ (Alfa Aesar 99.7%), and Y$_2$O$_3$ (Alfa Aesar 99.9%) were directly mixed with Ni powder (Alfa Aesar, ~325 mesh, 99.8% metal basis) to obtain Ni–BZY with a volume ratio of 40 : 60. Additional NiO (Alfa Aesar 99.9%, 2 wt% in BaCO$_3$, ZrO$_2$, and Y$_2$O$_3$) was added into the powder mixture as a sintering aid. The powder was then ball-milled in ethanol with ZrO$_2$ balls for 24 h and dried to obtain Ni–BZYNiO2-SSRS powder. BZY powder with 2 wt% NiO
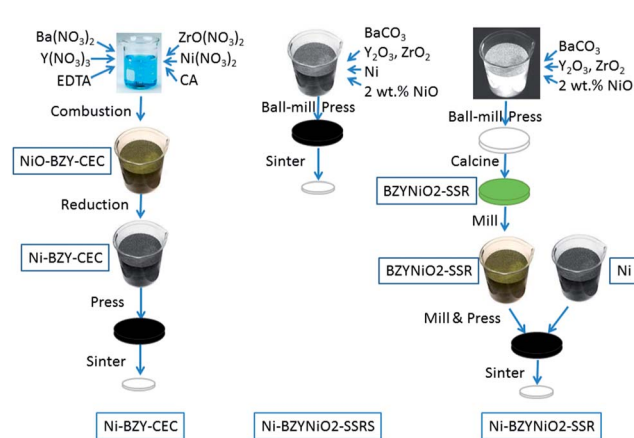

Fig. 1 Schematic of the different methods for fabrication of Ni–BZY membranes.

was also prepared using this method by skipping the addition of Ni (denoted as BZYNiO2-SSRS). BZY20 powder was prepared using this method by skipping the addition of Ni and NiO (denoted as BZY-SSRS). In the SSR method, stoichiometric amounts of $BaCO_3$, ZrO_2, Y_2O_3, and NiO (2 wt% in $BaCO_3$, ZrO_2, and Y_2O_3) were ball-milled in ethanol with ZrO_2 balls for 24 h. The powder was dried and pressed into pellets followed by calcination at 1200, 1300, and 1400 °C for 5, 10, and 10 h, respectively. The calcined pellets were crushed and carefully milled to obtain BZY powder with 2 wt% NiO (denoted as BZYNiO2-SSR), which was mixed with Ni powder in a volume ratio of 60 : 40 by using an agate mortar and pestle to obtain Ni–BZYNiO2-SSR powder. The abbreviations of the different samples are summarized in Table 1.

All Ni–BZY or Ni–BZYNiO2 powders were pressed into pellets with a 20 mm stainless steel die under a pressure of 100 MPa. The pellets were sintered at 1440 °C for 20 h in N_2 unless otherwise specified. To study the sintering behavior, different BZY, BZYNiO2, Ni–BZY, and Ni–BZYNiO2 powders were pressed into bars (length ∼8 mm) and investigated by dilatometry (Netzsch Dil-402). BZY and BZYNiO2 bars were sintered in air from room temperature to 1400 °C with a heating rate of 3 °C min^{-1} and a dwelling time of 10 h at 1400 °C. Ni–BZY and Ni–BZYNiO2 bars were sintered in N_2 from room temperature to 1440 °C with a heating rate of 3 °C min^{-1} and a dwelling time of 10 h at 1440 °C. The density of bars and pellets after sintering was measured by the Archimedes method in deionized water.

X-ray diffraction (XRD, Rigaku D/Max 2100, with Cu Kα radiation) analysis was used to identify the phases in the powders and pellets. Field emission scanning electronic microscopy (FESEM, Zeiss ultra plus) was used to study the microstructure and composition of the Ni–BZY membranes.

The membranes were tested in a set-up for hydrogen permeability measurements.[30] Both surfaces of the sintered membrane were polished with silicon carbide sandpaper (120, 320, and 600 grits) before measurement. The Ni–BZYNiO2 membrane was sealed using two glass rings to two vertical alumina tubes. To prevent exposure of the membrane to air, the edge of the membrane was first covered with 8252 glass powder (Schott) which was well-dispersed in terpineol, dried, and then covered by a ceramic-glass sealant (Aremco C552). Sealing was achieved by heating at 90, 130, 230, 1000 °C for 3, 3, 3 and 1 h, respectively. The feed gas was a mixture of H_2 balanced with ultra-high-purity (UHP) He and N_2 with a total flow rate of 100 mL min^{-1}. The sweep gas was 20 mL min^{-1} UHP N_2. The gas flow rates were controlled by using Apex mass flow

controllers (Schoonover). The composition of the exhaust gas from the sweep side was analyzed by using a calibrated gas chromatograph (GC, Agilent 7890A). The flow rate of the exhaust gas was measured by using a digital flow meter (Agilent ADM2000). The leakage due to incomplete sealing was checked by measuring He concentration in the sweep gas. No helium was detected, suggesting that an effective seal was obtained.

3 Results and discussion

3.1 Sintering behaviors of BZY, BZYNiO2 and Ni–BZY/BZYNiO2

Fig. 2 shows the sintering behaviors of BZY and BZYNiO2 bars prepared from three different methods during heating to 1400 °C at 3 °C min^{-1} followed by a dwelling time of 10 h. BZY-CEC shows a small shrinkage (∼8%), suggesting that its sinteractivity is poor. Surprisingly, BZY-SSRS shows expansion rather than shrinkage during the sintering process. The expansion may be due to the solid state reaction between $BaCO_3$, ZrO_2, and Y_2O_3 starting at ∼1000 °C, generating a large amount of gaseous CO_2 leading to expansion of the originally compacted bar sample. After the solid state reaction, the sample shrinks very slowly resulting in a total expansion of ∼4%, suggesting the refractory nature of the BZY material. Although BZYNiO2-SSRS also expands at ∼1000 °C, it starts to shrink very quickly at ∼1140 °C and finally reaches a drastic shrinkage of ∼30%, confirming the excellent sintering activity of NiO-added BZY powder prepared by the SSRS method and the effectiveness of NiO as the sintering aid as reported by Tong et al.[26,27] BZY-NiO2-SSR only shrinks by 13%, probably because the powder has been calcined at 1300 °C for 10 h to complete the solid state reaction to obtain the BZY phase. These results suggest that neither the solid state reactive sintering method nor the combustion method were effective in the densification of BZY ceramics. However, the use of NiO as a sintering aid can significantly promote the sintering of BZY ceramics both in the solid state reaction and solid state reactive sintering methods.

Table 1 List of abbreviations for materials

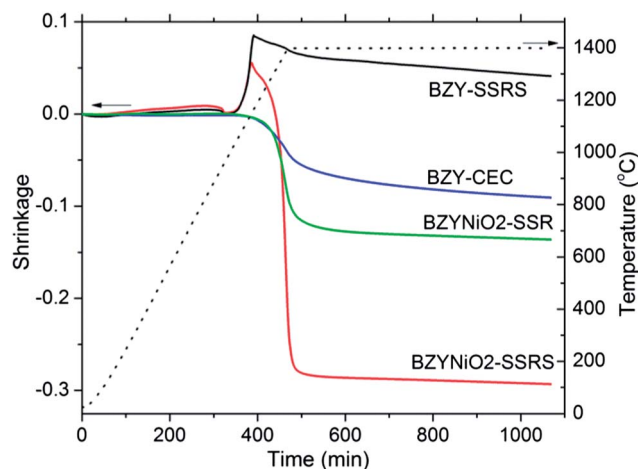| Sample abbreviations	Method	2 wt% NiO added?
BZY-CEC	CEC	No
BZY-SSRS	SSRS	No
BZYNiO2-SSRS	SSRS	Yes
BZYNiO2-SSR	SSR	Yes
Ni–BZY-CEC	CEC	No
Ni–BZYNiO2-SSRS	SSRS	Yes
Ni–BZYNiO2-SSR	SSR	Yes

Fig. 2 Sintering behaviors of BZY and BZYNiO2 ceramics prepared from different methods.

Besides, the expansion process and drastic shrinkage can cause the delamination of the BZYNiO2-SSRS film from the anode, making it unsuitable for application as an electrolyte for SOFCs. However, BZYNiO2-SSR is not limited by these factors, and thus may be used as an electrolyte for SOFCs.

The SEM images in Fig. 3 show that BZY-SSRS and BZY-CEC are still very porous with very small grain sizes (∼300 and 150 nm, respectively). However, both BZYNiO2-SSRS and BZY-NiO2-SSR are very dense with grain sizes around 1 μm. Different microstructures of the sintered samples from the different fabrication methods show that SSRS is not the prerequisite for densification. Rather, the use of NiO as a sintering aid resulted in improved sample densification irrespective of the processing route utilized. Tong *et al.* found that BaY_2NiO_5 formed *via* a reaction between $BaCO_3$, Y_2O_3, and NiO can effectively promote the densification and grain growth of BZY.[26] In the present work, large grains were observed in BZYNiO2-SSRS, which were determined to be BaY_2NiO_5 by XRD and SEM-EDX (Fig. 5 and S1†). BaY_2NiO_5 was formed *in situ* during the sintering process and agglomerates to act as the sintering center.[26] In BZYNiO2-SSR, BaY_2NiO_5 was formed during the calcination process and was subsequently broken down into small particles during the crushing and milling process. These results suggest that the SSR method works as well as the SSRS method for the sintering and grain growth of BZY. Because of the excellent sintering activity of BZYNiO2-SSRS and BZYNiO2-SSR, they were subsequently mixed with Ni to prepare a Ni–BZYNiO2 composite membrane. Recently, Bi *et al.* have reported the one-pot method to prepare sinteractive NiO–BZY powder.[23] Since NiO–BZY powder can be reduced to a Ni–BZY powder, a Ni–BZY membrane was also prepared by the CEC method in this work to provide a basis for comparison.

Fig. 4 shows the sintering behaviors of the Ni–BZY and Ni–BZYNiO2 composites in N_2, which can preserve most Ni from oxidation and NiO from reduction in raw materials. Similar to the sintering behavior of the corresponding BZYNiO2 phases, Ni–BZYNiO2-SSR (BZYNiO2 first calcined at 1300 °C for 10 h) shows a smaller shrinkage (∼7%) than Ni–BZYNiO2-SSRS

Fig. 4 The sintering behaviors of Ni−BZY and Ni−BZYNiO2 composites prepared by different methods.

(∼17%). The relative densities of Ni–BZYNiO2-SSRS and Ni–BZYNiO2-SSR pellets sintered at 1440 °C for 20 h in N_2 were 96.2% and 97.8%, respectively, suggesting that both samples were dense after sintering. These membranes were also gas tight, indicating there was no open porosity present. The Ni–BZY-CEC shows the largest shrinkage among all the three methods. However, the sintered sample cracked into small pieces after the dilatometry test, indicating the poor mechanical strength of the sample, which originates from the low bonding strength between the fine spherical particles. The large shrinkage observed from the dilatometry result was due to disintegration of the sample under a pushing force rather than the shrinkage from sintering. The sintering behaviors of the BZY/BZYNiO2 ceramic and the Ni–BZY/BZYNiO2 composite suggest that the introduction of NiO as a sintering aid is the prerequisite for their densification.

3.2 Phase composition of the Ni–BZY/BZYNiO2 samples before and after sintering in N_2

Fig. 5 shows the XRD patterns of Ni–BZY pellets fabricated from three different methods before and after sintering at 1440 °C for 20 h in N_2. The phase compositions in these patterns are summarized in Table 2. Before sintering, the Ni–BZY-CEC contained only BZY and Ni phases, which were formed after calcination and reduction, respectively. Ni–BZYNiO2-SSRS contained all the raw materials, since it was just a mixture of these powders. The Ni–BZYNiO2-SSR contained Ni, BZY and a small amount of BaY_2NiO_5, whereas BZY and BaY_2NiO_5 were formed after the solid state reaction at 1300 °C for 10 h. After sintering, all the pellets turned into a mixture of Ni and BZY, except for a minor difference in the form of the secondary phases. The Ni–BZY-CEC contained a small amount of Y_2O_3, probably due to the evaporation of BaO during high temperature sintering, which is commonly observed in sintered BZY samples.[31] The Ni–BZYNiO2-SSRS and Ni–BZYNiO2-SSR contained a small amount of BaY_2NiO_5, which has been reported as the actual sintering aid and does not completely decompose
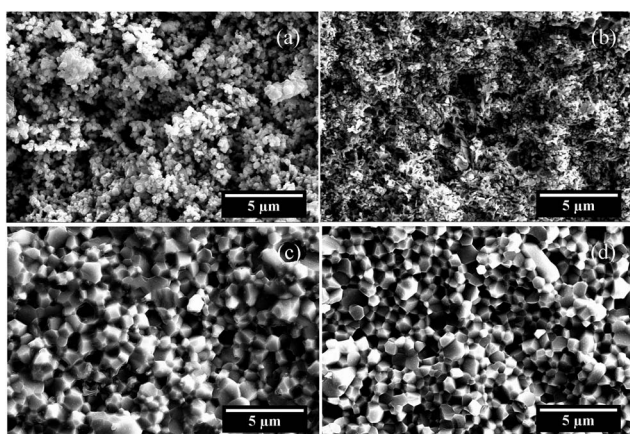

Fig. 3 Cross-section SEM images of BZY and BZYNiO2 ceramics sintered at 1400 °C for 10 h in air. (a) BZY-SSRS, (b) BZY-CEC, (c) BZYNiO2-SSR, and (d) BZYNiO2-SSRS.
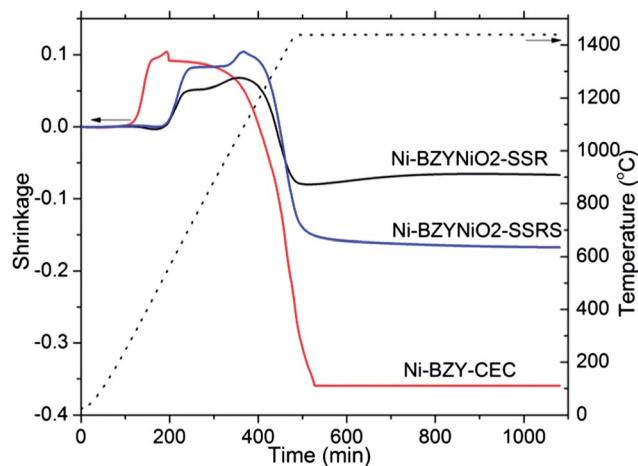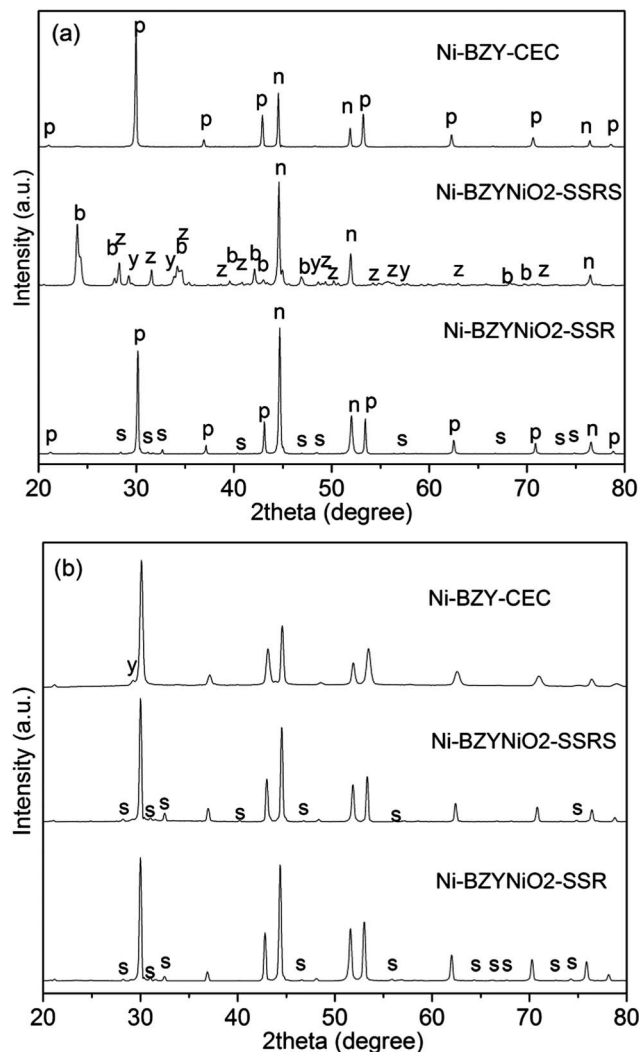
Fig. 5 XRD patterns of Ni–BZY/BZYNiO2 membranes before (a) and after (b) sintering at 1440 °C for 20 h in N_2. p: BZY, n: Ni, b: $BaCO_3$, z: ZrO_2, y: Y_2O_3, and s: BaY_2NiO_5.

during sintering.[26,27] It was also noticed that the sintered Ni–BZYNiO2-SSRS samples contained more BaY_2NiO_5 than the sintered Ni–BZYNiO2-SSR samples. Ni–BZYNiO2-SSRS and Ni–BZYNiO2-SSR have similar phase composition, which leads to their similar sintering behaviors. However, the difference in the amount of BaY_2NiO_5 may lead to differences in their microstructure which may impact hydrogen separation membrane performance.

Table 2 Summary of phase compositions before and after sintering

Sample identification	Main phases	Minor phases
Ni–BZY-CEC-before	Ni, BZY	N/A
Ni–BZYNiO2-SSRS-before	Ni, $BaCO_3$, ZrO_2, Y_2O_3, NiO	N/A
Ni–BZYNiO2-SSR-before	Ni, BZY	BaY_2NiO_5
Ni–BZY-CEC-after	Ni, BZY	Y_2O_3
Ni–BZYNiO2-SSRS-after	Ni, BZY	BaY_2NiO_5
Ni–BZYNiO2-SSR-after	Ni, BZY	BaY_2NiO_5

3.3 Microstructure of the sintered Ni–BZY/BZYNiO2 composite membranes

Table 3 tabulates the results of the SEM study and density measurement performed on Ni–BZY and Ni–BZYNiO2 composites prepared by different methods. In Ni–BZY-CEC (Fig. 6a), BZY and Ni grain sizes are very small, only ~0.25 nm and ~1–3 μm, respectively. Although Ni–BZY powder from the CEC method is very sinterative, it does not contain the BaY_2- NiO_5 phase which was demonstrated to assist the growth of BZY grains. Consequently, the Ni–BZY-CEC membrane was dense (holes in the image are pull-outs of Ni particles) with small BZY grains. Furthermore, the obtained Ni–BZY-CEC membrane is not conductive at room temperature, suggesting that the Ni particles did not form a percolating network throughout the membrane thickness. Therefore, the permeation flux from the Ni–BZY composite membrane prepared from the CEC method was expected to be low. The Ni–BZYNiO2-SSRS sample (Fig. 6b) is also very dense with much larger BZY and Ni grains (~1–2 μm and ~10 μm, respectively). The membrane was conductive at room temperature, indicating that a connective Ni network was formed.

Unlike the Ni–BZYNiO2 membranes prepared by the solid state reactive sintering method, there was an additional calcination process for BZYNiO2 powder in the solid state reaction method. In order to study the effect of calcination conditions on the microstructure of Ni–BZYNiO2-SSR membranes, BZYNiO2 powders were first calcined at 1200 °C for 5 h, 1300 °C for 10 h, and 1400 °C for 10 h. Fig. 7 shows the SEM images of these Ni–BZYNiO2-SSR membranes. The BZY grain size increased when calcination temperature increased from 1200 to 1300 °C, and remained stable when the calcination temperature was further increased to 1400 °C. For the sample first calcined at 1400 °C for 10 h, as shown in a low magnification image (Fig. 7d), there are

Table 3 Summary of microstructure analysis and density measurement of Ni–BZY and Ni–BZYNiO2 composites

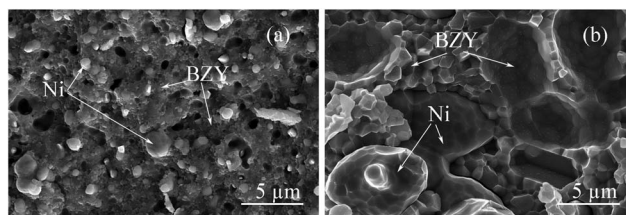| Sample identification	Size of Ni (μm)	Size of BZY (μm)	Relative density
Ni–BZY-CEC	~1–3	~0.25	93.5%
Ni–BZYNiO2-SSRS	~10	~1–2	96.2%
Ni–BZYNiO2-SSR-1200	~10	~0.7–1	92.6%
Ni–BZYNiO2-SSR-1300	~10	~1–2	97.8%
Ni–BZYNiO2-SSR-1400	~10	~1–2	89.8%

Fig. 6 Cross-section SEM images of Ni–BZY-CEC (a) and Ni–BZY-NiO2-SSRS (b) after sintering at 1440 °C for 20 h in N_2.
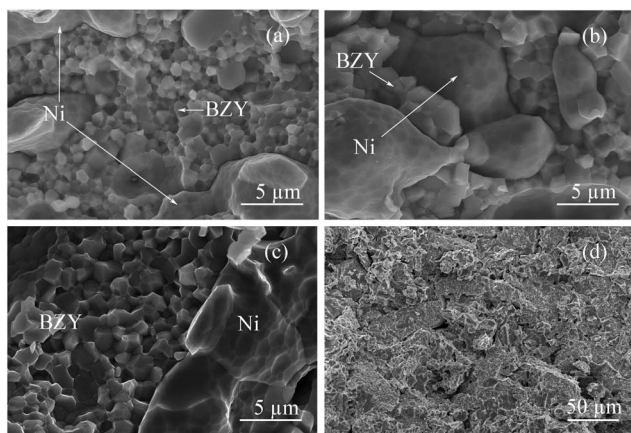
Fig. 7 Cross-section images of Ni–BZYNiO2-SSR using BZYNiO2 calcined at 1200 °C for 5 h (a), 1300 °C for 10 h (b), 1400 °C for 10 h (c), and 1400 °C for 10 h in low magnification (d).

some ceramic lumps (length up to ∼70 μm) with slits around them, which agrees well with its low relative density. After calcination at 1300 °C, BZYNiO2 is still porous with sub-micrometer-sized particles (Fig. S2†). After calcination at 1400 °C for 10 h, the BZYNiO2 pellet was already dense (Fig. 3d), and the crushing and milling process probably could not completely break down the well-sintered ceramic, leaving some ceramic lumps. Unlike the fine ceramic powders which are sinteractive and can stack closely, these lumps are not sinter-active and stack loosely, leading to the formation of slits and porosity. Since low calcination temperature (1200 °C) leads to small BZY grains, and high calcination temperature (1400 °C) leads to a porous membrane, the optimal calcination conditions were found to be 1300 °C for 10 h for the Ni–BZYNiO2-SSR membranes.

A 2-step sintering process was employed to study the chemical stability of composite Ni–BZY membranes in a H_2 atmosphere. Ni–BZYNiO2-SSRS and Ni–BZYNiO2-SSR were sintered at 1440 °C for 20 h in N_2 followed by 20 h in 5% H_2/N_2. Fig. 8 shows their cross-section SEM images. Ni–BZYNiO2-SSRS became rather porous (relative density = 86.2%) while the Ni–BZYNiO2-SSR was still very dense (relative density = 97.4%), suggesting that the Ni–BZYNiO2-SSRS composite membranes are not suitable for applications in hydrogen separation. The Ni–BZYNiO2-SSRS membrane was dense after sintering in N_2 (Fig. 6b) but turns porous after further sintering in 5% H_2/N_2,
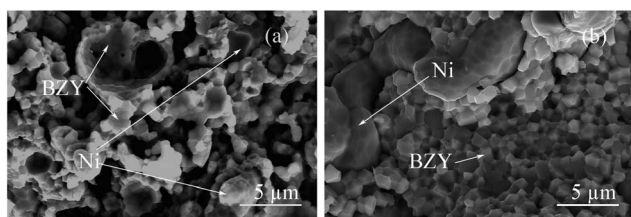

Fig. 8 Cross-section SEM images of Ni–BZYNiO2-SSRS (a) and Ni–BZYNiO2-SSR (b) sintered at 1440 °C for 20 h in N_2 and 10 h in 5% H_2/N_2.

indicating that it contains phases that are unstable in reducing atmospheres. The phase composition was investigated to find the cause of the porosity, as discussed in the following section.

3.4 Differences in the sintering mechanism between Ni–BZYNiO2-SSR and Ni–BZYNiO2-SSRS membranes

Fig. 9 shows the XRD patterns of Ni–BZYNiO2-SSRS and Ni–BZYNiO2-SSR after sintering in N_2 and then in 5% H_2. Ni–BZYNiO2-SSRS contains significantly more Y_2O_3 than Ni–BZYNiO2-SSR. Because Y_2O_3 is the residue from the decomposition of BaY_2NiO_5 in H_2, this agrees well with the XRD results in Fig. 5 that Ni–BZYNiO2-SSRS samples contained more BaY_2NiO_5 than Ni–BZYNiO2-SSR samples when sintered in N_2. Ni–BZYNiO2-SSRS should have less BaY_2NiO_5 because the raw materials are diluted by Ni and the sites available for the solid state reaction are less. Ni–BZYNiO2-SSR has no such problem because BaY_2NiO_5 is already formed before mixing with Ni (Fig. 5a). However, the results show that Ni in Ni–BZYNiO2-SSRS promotes the formation of BaY_2NiO_5. Therefore, we think that a certain amount of Ni may be oxidized in this sample, leading to more NiO phases than expected. Since Ni itself can provide NiO, the addition of NiO may not be necessary. In order to verify this, Ni–BZY-SSR was synthesized under the same conditions by mixing Ni and BZY prepared from the SSR method at 1300 °C for 10 h. The cross-section SEM image of the Ni–BZY membrane sintered in N_2 and then in 5% H_2 is shown in Fig. 10. The membrane shows a very dense microstructure with a high relative density of 98.4%, similar to that of Ni–BZYNiO2-SSR. The grain size of BZY is also ∼1–2 μm. This confirms our hypothesis that NiO from oxidation of Ni can act as a sintering aid. The formation of BaY_2NiO_5 is due to the reaction among NiO (from oxidation of Ni), residual $BaCO_3$, and Y_2O_3. The existence of $BaCO_3$ was confirmed by XRD from the BZY pellet after calcination at 1300 °C for 10 h (See Fig. S3†). During heating up to 1300 °C, $BaCO_3$ decomposed to CO_2 and BaO
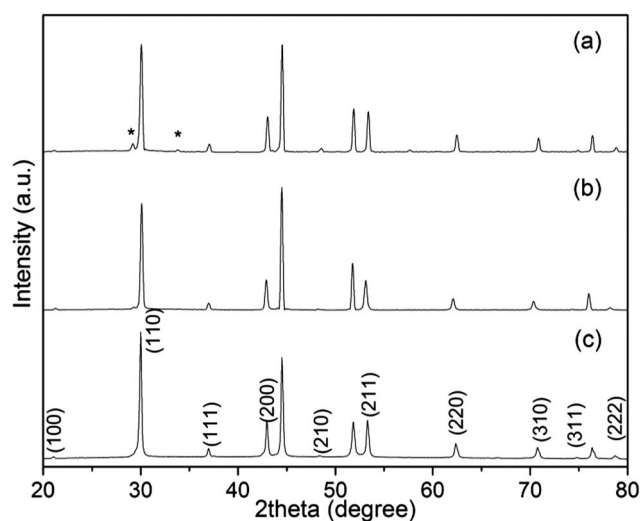

Fig. 9 XRD patterns of Ni–BZYNiO2-SSRS (a) and Ni–BZYNiO2-SSR (b and c) sintered at 1440 °C for 20 h in N_2 and 10 h in 5% H_2/N_2 (a and b) or 20 h in N_2 and 20 h in 5% H_2/N_2 (c). *: Y_2O_3.
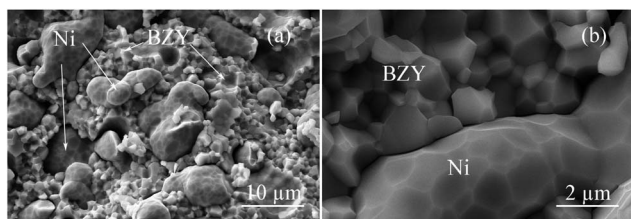
Fig. 10 SEM images of Ni–BZY20-SSR sintered at 1440 °C for 20 h in N_2 and 20 h in 5% H_2/N_2. (a) Low magnification and (b) high magnification.

reacted with ZrO_2 and Y_2O_3 forming BZY. However, due to the inhomogeneous mixing and large particles of the raw material, the reaction was incomplete. The residual BaO would react with CO_2 in air during the cooling process forming $BaCO_3$. The same mechanism works in Ni–BZYNiO2-SSRS because there are large amounts of $BaCO_3$, Y_2O_3, NiO, and NiO from oxidation of Ni.

There are two main differences between SSRS and SSR methods. First, in the SSRS method, besides the reaction among $BaCO_3$, Y_2O_3, and original NiO forming BaY_2NiO_5, the oxidation of Ni to NiO provides additional NiO which reacts with plenty of unreacted $BaCO_3$ and Y_2O_3 generating a significant amount of BaY_2NiO_5. In the SSR method using NiO as the sintering aid, most raw materials are transformed into BZY20 and partial raw materials are transformed into BaY_2NiO_5. The oxidation of Ni does not contribute to more BaY_2NiO_5 because there are no more $BaCO_3$ and Y_2O_3 after the SSR reaction. The amount of BaY_2NiO_5 is merely determined by the amount of NiO sintering aid during the calcination process in the SSR method. Therefore, there is much more BaY_2NiO_5 in the SSRS method than in the SSR method. Second, BaY_2NiO_5 is *in situ* generated during the SSRS process and is not evenly distributed. Much of it is agglomerated in certain spots forming big particles (Fig. 3d and S1†). After reduction, these big BaY_2NiO_5 particles will decompose forming big pores. In the SSR method, there are additional crushing, milling, and mixing processes. BaY_2NiO_5 is broken into small pieces and distributed evenly before sintering. After reduction, the small pores caused by decomposition of small BaY_2NiO_5 particles can be eliminated during extended sintering. Fig. 9 also shows that the extension of sintering time in 5% H_2/N_2 from 10 to 20 h leads to the disappearance of the already low Y_2O_3 peaks in the Ni–BZYNiO2-SSR membrane, indicating that Y_2O_3 may be dissolved into the BZY lattice under these conditions.

Based on our results, it can be concluded that the introduction of NiO (directly added or *in situ* formed from Ni) rather than the SSRS method is the key parameter for the densification of BZY ceramic and Ni–BZY composite membranes. The SSRS method leads to the formation of a large amount of BaY_2NiO_5 agglomerates while the SSR method avoids the formation of a large amount of BaY_2NiO_5. Besides, the additional milling process in the SSR method can break down the agglomerates. After reduction, the decomposition of BaY_2NiO_5 leads to significant porosity in Ni–BZYNiO2-SSRS but not in the Ni–BZYNiO2-SSR membrane. Therefore, a dense Ni–BZY membrane with large BZY grains can only be obtained by the SSR method with the addition of NiO as the sintering aid. Most importantly,

the introduction of NiO is flexible. It can be added before or after the SSR reaction, directly by inclusion of NiO or indirectly by oxidation of Ni. These findings are also important for the development of the NiO–BZY anode for intermediate temperature solid oxide fuel cells. Since large-grained BZY possesses high proton conductivity and chemical stability in H_2O, CO_2, and H_2S, it is expected to be an excellent anode component. In comparison, conventional doped $BaCeO_3$ or CeO_2 are unstable in one or all of these gas atmospheres. The sinterative NiO–BZY anode can be prepared by the SSR method, which costs only a fraction of the one-pot combustion method due to the inexpensive raw materials and ease of processing.[23]

3.5 Hydrogen permeation flux of the Ni–BZYNiO2-SSR membrane

Fig. 11 shows the hydrogen flux of a 0.44 mm-thick Ni–BZY-NiO2-SSR membrane. The flux increases with temperature between 825 and 900 °C. The fluxes at 900 °C in wet 20 and 40% H_2 are 3.4 and 4.3 $\times 10^{-8}$ mol cm^{-2} s^{-1}, respectively. Further improvement of flux is possible through optimization of the synthesis process and reduction of membrane thickness. As a comparison, 0.9 mm-thick $BaZr_{0.85}Y_{0.15}Mn_{0.05}O_{3-\delta}$ and $(Nd_{5/6}La_{1/6})_{5.5}WO_{12-\delta}$ membranes only show a flux of 3.0 and 5.6 $\times 10^{-9}$ mol cm^{-2} s^{-1} in wet 50% H_2 at 900 °C, respectively.[9,14] It is also significantly higher than that of the Ni–$La_{0.4875}Ca_{0.0125}Ce_{0.5}O_{2-\delta}$ membrane (2.1 $\times 10^{-8}$ mol cm^{-2} s^{-1} for a 0.51 mm-thick membrane at 900 °C in wet 20% H_2).[10] In general, the Ni–BZY membrane shows the highest hydrogen flux among non-$BaCeO_3$-based membranes through the combination of large BZY grains and high bulk proton conductivity. However, it is still significantly lower than that of the Ni–$BaZr_{0.1}Ce_{0.7}Y_{0.1}Yb_{0.1}O_{3-\delta}$ (Ni–BZCYYb) membrane (7.6 $\times 10^{-8}$ mol cm^{-2} s^{-1} for a 0.40 mm-thick membrane at 900 °C in wet 20% H_2).[30] There might be several reasons for this: first, the
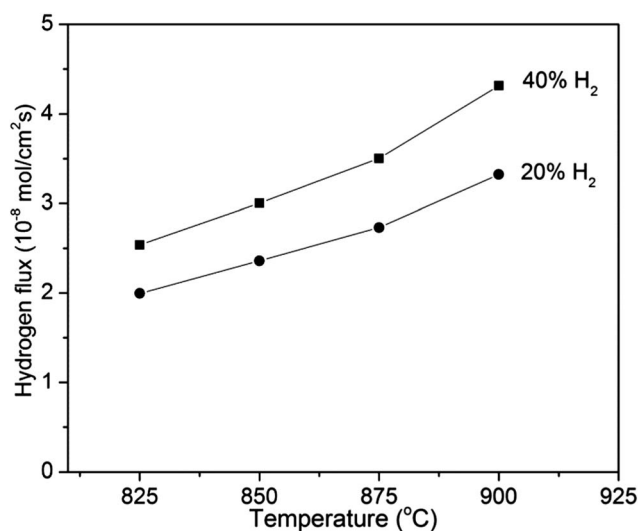

Fig. 11 Temperature dependence of hydrogen permeation flux for a 0.44 mm-thick Ni–BZYNiO2-SSR membrane. Feed gas is 100 mL min^{-1} wet gas containing H_2, N_2, and He. Sweep gas is 20 mL min^{-1} N_2.

hydrogen surface exchange rate on the Ni–BZY membrane may be significantly slower than that of the Ni–BZCYYb membrane. The large BZY grain size is beneficial for the proton conductivity but reduces the area of gas-BZY–Ni triple phase boundaries. However, hydrogen can be adsorbed on Ni, diffuses to the boundary of Ni and BZY phases, and then dissociates into protons and electrons. The protons are transferred into the BZY phase and Ni collects the electrons.[32] The small area of TPBs should not be the obstacle for hydrogen surface exchange. Second, the use of the NiO sintering aid may lead to change in the chemical composition of BZY, which can reduce its proton conductivity. Further studies are required to verify these possibilities and find corresponding solutions. Besides, the chemical stability of the Ni–BZY membrane in wet CO_2 is crucial for its application in hydrogen separation after steam methane reforming. We are currently studying performance stability of the Ni–BZY membranes in wet CO_2 and the findings will be reported in due course.

4 Conclusions

For the first time, dense Ni–BZY membranes were fabricated for hydrogen separation using high performance, chemically stable but highly refractory BZY. Three methods were employed to fabricate dense Ni–BZY membranes with large BZY grains. The combined EDTA-citric method (CEC) method produced dense membranes, but exhibited small BZY grain size ($\sim$0.25 μm) due to the absence of an intermediate phase BaY_2NiO_5 as a sintering aid. The solid state reactive sintering (SSRS) method resulted in dense membranes with large BZY grains, however the membrane became porous after reduction. It was found that partial Ni could be oxidized to NiO during the sintering process, generating more BaY_2NiO_5 than expected. BaY_2NiO_5 agglomerated and decomposed after in H_2, resulting in the observed porosity. Of the methods investigated, only the solid state reaction (SSR) method was able to produce dense Ni–BZY membranes with large BZY grains after the sintering in N_2, followed by reduction in H_2. The additional solid state reaction and milling processes in the SSR method avoid the generation of excessive large BaY_2NiO_5 particles. The hydrogen flux of the Ni–BZYNiO2-SSR membrane was significantly higher than that of the single-phase BZY membrane and other stable ceramic membranes, making it very attractive for applications in hydrogen separation.

Acknowledgements

Notes and references

1 N. Z. Muradov and T. N. Veziroglu, *Int. J. Hydrogen Energy*, 2005, **30**, 225–237.

2 M. V. Twigg, *Catalyst handbook*, Wolfe Publishing Ltd, London, 1997.

3 N. W. Ockwig and T. M. Nenoff, *Chem. Rev.*, 2007, **107**, 4078–4110.

4 K. Brinkman, E. Fox, P. Korinko, D. Missimer, T. Adams and D. Su, *J. Membr. Sci.*, 2011, **378**, 301–307.

5 S. Fang, L. Bi, X. Wu, H. Gao, C. Chen and W. Liu, *J. Power Sources*, 2008, **183**, 126–132.

6 C. Zuo, T. H. Lee, S.-J. Song, L. Chen, S. E. Dorris, U. Balachandran and M. Liu, *Electrochem. Solid-State Lett.*, 2005, **8**, J35–J37.

7 C. Zuo, S. E. Dorris, U. Balachandran and M. Liu, *Chem. Mater.*, 2006, **18**, 4647–4650.

8 S. Escolástico, V. B. Vert and J. M. Serra, *Chem. Mater.*, 2009, **21**, 3079–3089.

9 S. Escolástico, C. Solís and J. M. Serra, *Int. J. Hydrogen Energy*, 2011, **36**, 11946–11954.

10 S. Fang, L. Bi, L. Yan, W. Sun, C. Chen and W. Liu, *J. Phys. Chem. C*, 2010, **114**, 10986–10991.

11 W. Xing, G. E. Syvertsen, T. Grande, Z. Li and R. Haugsrud, *J. Membr. Sci.*, 2012, **415–416**, 878–885.

12 W. Sun, Z. Shi and W. Liu, *J. Electrochem. Soc.*, 2013, **160**, F585–F590.

13 K. D. Kreuer, *Annu. Rev. Mater. Res.*, 2003, **33**, 333–359.

14 S. Escolastico, M. Ivanova, C. Solis, S. Roitsch, W. A. Meulenberg and J. M. Serra, *RSC Adv.*, 2012, **2**, 4932–4943.

15 K. D. Kreuer, St. Adams, W. Munch, A. Fuchs, U. Klock and J. Maier, *Solid State Ionics*, 2001, **145**, 295–306.

16 S. Imashuku, T. Uda and Y. Awakura, *Electrochem. Solid-State Lett.*, 2007, **10**, B175–B178.

17 H. G. Bohn and T. Schober, *J. Am. Ceram. Soc.*, 2000, **83**, 768–772.

18 P. Babilo, T. Uda and S. M. Haile, *J. Mater. Res.*, 2007, **22**, 1322–1330.

19 F. Iguchi, Y. Nagao, N. Sata and H. Yugami, *Solid State Ionics*, 2011, **192**, 97–100.

20 Y. Yamazaki, R. Hernandez-Sanchez and S. M. Haile, *Chem. Mater.*, 2009, **21**, 2755–2762.

21 F. Iguchi, N. Sata and H. Yugami, *J. Mater. Chem.*, 2010, **20**, 6265–6270.

22 C. Chen, C. E. Danel and S. Kim, *J. Mater. Chem.*, 2011, **21**, 5435–5442.

23 L. Bi, E. Fabbri, Z. Sun and E. Traversa, *Energy Environ. Sci.*, 2011, **4**, 1352–1357.

24 W. G. Coors, in *Advances in Ceramics – Synthesis and Characterization, Processing and Specific Applications*, ed. C. Sikalidis, InTech, Croatia, 2011, ch. 21, pp. 479–500.

25 D. Pergolesi, E. Fabbri, A. D'Epifanio, E. Di Bartolomeo, A. Tebano, S. Sanna, S. Licoccia, G. Balestrino and E. Traversa, *Nat. Mater.*, 2010, **9**, 846–852.

26 J. Tong, D. Clark, L. Bernau, M. Sanders and R. O'Hayre, *J. Mater. Chem.*, 2010, **20**, 6333–6341.

27 J. Tong, D. Clark, M. Hoban and R. O'Hayre, *Solid State Ionics*, 2010, **181**, 496–503.

28 S. Nikodemski, J. Tong and R. O'Hayre, *Solid State Ionics*, 2013, **253**, 201–210.

5832 | *J. Mater. Chem. A*, 2014, **2**, 5825–5833

This journal is © The Royal Society of Chemistry 2014

29 L. Bi, E. Fabbri, Z. Sun and E. Traversa, *J. Electrochem. Soc.*, 2011, **158**, B797–B803.

30 S. Fang, K. Brinkman and F. Chen, *ACS Appl. Mater. Interfaces*, 2014, **6**, 725–730.

31 W. Sun, L. Yan, Z. Shi, Z. Zhu and W. Liu, *J. Power Sources*, 2010, **195**, 4727–4730.

32 E. Fabbri, D. Pergolesi and E. Traversa, *Sci. Technol. Adv. Mater.*, 2010, **11**, 044301.